A study of the freshwater discharge from the Amazon River into the tropical Atlantic using multi-sensor data

Young-Heon Jo,[1] Xiao-Hai Yan,[1,2] Brian Dzwonkowski,[1] and W. Timothy Liu[3]

Received 26 October 2004; revised 3 December 2004; accepted 23 December 2004; published 25 January 2005.

[1] We study freshwater discharge from the Amazon River into the tropical Atlantic using monthly mean multi-sensor data from September 1997 to July 2003. In order to demonstrate freshwater discharge, we used chlorophyll concentration (Chl_a) and diffuse attenuation coefficient (DAC) measured by the Sea-viewing Wide Field-of-view Sensor (SeaWiFS), and salt steric height anomaly ($\Delta\eta'_S$) derived from Integrated Multi-Sensor Data Analysis (IMSDA). IMSDA was obtained from estimating the long term-time series of $\Delta\eta'_S$ by removing the thermal steric height anomaly (η'_T) from altimetry data. Comparisons of long-term time series of $\Delta\eta'_S$, Chl_a, and DAC were made with mooring data at 8°N, 38°W, which were highly correlated. There are three- to five-month lags between the Amazon River discharge and 4°N latitude estimated from latitude-time diagram derived from SeaWiFS measurements.

Citation: Jo, Y.-H., X.-H. Yan, B. Dzwonkowski, and W. T. Liu (2005), A study of the freshwater discharge from the Amazon River into the tropical Atlantic using multi-sensor data, *Geophys. Res. Lett.*, *32*, L02605, doi:10.1029/2004GL021840.

1. Introduction

[2] The importance of the salinity variation due to the river outflow into the oceans cannot be emphasized enough. For instance, the Amazon River is the largest river system in the world, and contributes about 6×10^{12} m^3 of freshwater and 1 Gtyr^{-1} of sediment discharge [*Dagg et al.*, 2004] to the tropical Atlantic. This freshwater is about 16% of the annual discharge into the world's oceans [*Baumgartner and Reichel*, 1975]. *Hellweger and Gordon* [2002] studied the Amazon River water into the Caribbean Sea using historical Sea Surface Salinity (SSS). However, the estimation of the freshwater outflow was solely dependent on in-situ measurements which spatially undersample the region of interest. Consequently, several questions arise, particularly whether we can estimate salinity variation due to the Amazon River discharge into the tropical Atlantic and whether we can analyze the trajectory of the freshwater after it leaves the North Brazil Current (NBC) using satellite multi-sensor data?

[3] The purpose of the study is to answer the two questions above. Specifically, we will demonstrate whether the estimates of variability of freshwater discharge from the Amazon River into the tropical Atlantic can be estimated directly, indirectly, or both from satellite remote sensing data. We considered chlorophyll concentration (Chl_a) and diffuse attenuation coefficient (DAC) measured by Sea-viewing Wide Field-of-view Sensor (SeaWiFS) as indirect evidence of freshwater discharge from the Amazon River, and by the mooring data as direct evidence. In order to obtain the dynamic signal of freshwater discharge in the tropical Atlantic, we estimated the contribution of the salinity variation in the altimeter measurements after removing the thermal steric height. This paper is organized as follows. The data and methodology are introduced in Section 2. The standard deviation (STD) of the thermal steric height (η_T) and the salt steric height (η_S) were estimated using Levitus 94 climatology data [*Levitus et al.*, 1994] to argue that η_S is more dominant than η_T in the western tropical Atlantic. In addition, we compared them with the annual mean Chl_a and DAC measured by SeaWiFS in Section 3. We estimated the salt steric height anomaly ($\Delta\eta'_S$) derived from IMSDA and compared it with both mooring data and SeaWiFs measurements. Finally, we estimated a lag between the Amazon River discharge and 4°N latitude using latitude-time diagram derived from SeaWiFS measurements in Section 4. Section 5 contains the discussion and conclusion.

2. Data and Methodology

[4] Monthly altimeter anomaly (η'_{Alt}) from the TOPEX/Poseidon (T/P) and Jason for the time period of September 1997 to July 2003 was obtained from the University of Texas Center for Space Research (UT/CSR). The sea surface height anomaly was obtained by removing a mean surface height, and we proceeded with instrument corrections (ionosphere, wet and dry troposphere, and electromagnetic bias) and geophysical corrections (tides and inverted barometer) [*Chambers et al.*, 1997].

[5] In order to estimate the thermal steric height using expandable bathythermographs (XBT) in the upper layer, we calculated it using monthly mean vertical temperature data acquired from the Joint Environmental Data Analysis (JEDA) Center. The variabilities of the temperatures were integrated through the water column to a depth of 400 m from September 1997 to July 2003 to estimate thermal steric height anomaly (η'_T):

$$\eta'_T = \int_{-400}^{0} \alpha \Delta T' \mathrm{d}z = \int_{-400}^{0} \alpha\left(T - \overline{T}\right)\mathrm{d}z, \qquad (1)$$

where α is the thermal expansion coefficient at constant pressure (P) and salinity (S), $\alpha = \left|\frac{1}{\rho_0}\frac{d\rho}{dT}\right|_{P,S}$. The temperature variabilities/anomalies ($\Delta T'$) were obtained by removing the

[1]Center for Remote Sensing, Graduate College of Marine Studies, University of Delaware, Newark, Delaware, USA.
[2]Also at Ocean Remote Sensing Institute, Ocean University of China, Qingdao, China.
[3]Jet Propulsion Laboratory, California Institute of Technology, Pasadena, California, USA.

0094-8276/05/2004GL021840$05.00

climatology ($\overline{T}$) from a long-term-time series of temperature measurements (T).

[6] Similar to η'_T, the salt steric height anomaly (η'_S) can be obtained by integrating through the water column to a depth of 400 m.

$$\eta'_S = -\int_{-400}^{0} \beta \Delta S' dz = -\int_{-400}^{0} \beta(S - \overline{S}) dz, \qquad (2)$$

where β is the salt expansion coefficient at constant pressure (P) and temperature (T), i.e., $\beta = \left|\frac{1}{\rho_0}\frac{d\rho}{dS}\right|_{P,T}$. The salinity anomalies ($\Delta S'$) were obtained by removing climatology ($\overline{S}$) from salinity measurements (S).

[7] For Chl_a and DAC, the data has been obtained from GES Distributed Active Archive Center (DAAC). The web-site is given by http://daac.gsfc.nasa.gov/data/dataset/SEAWIFS/index.html. The level 3 (L3) Standard Mapped Image (SMI) files that were acquired are image representations of the L3 binned data products. The "bins" correspond to grid cells on a global grid, each cell is approximately 81 square kilometers in size (http://daac.gsfc.nasa.gov/CAMPAIGN_DOCS/BRS_SRVR/seawifsbrs_info.html).

[8] In order to validate the estimation of the salinity variation using IMSDA, we used SSS acquired from the Pilot Research Moored Array in the Tropical Atlantic (PIRATA). The web-site is given by http://www.pmel.noaa.gov/pirata/.

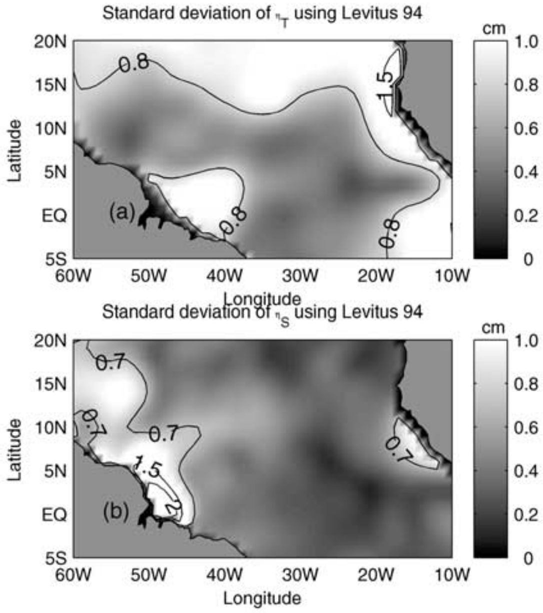

Figure 1. (a) Standard deviation of the thermal steric height (η_T) and (b) the salt steric height (η_T) using Levitus 94 climatological temperature and salinity data in the tropical Atlantic. The η_T and η_S were estimated using the first term in the right hand side of equations (1) and (2), respectively.

3. Evidence of Freshwater Discharge From the Amazon River in the Tropical Atlantic

[9] In order to examine annual variability of heat and salinity, we computed the STD of η_T derived from the first term ($\int_{-400}^{0} \alpha T dz$) in the right hand side of equation (1), and η_S derived from the first term($-\int_{-400}^{0} \beta S dz$) in the right hand side of equation (2) using Levitus 94 climatology data. The STD of these time series is analogous to the long term-times series of the altimetry and the XBT temperature anomalies used to estimate variability of heat. The STD of η_T and η_S suggests that η_S is more dominant than the thermal steric height as shown in Figures 1a and 1b. There is an order of over 3 cm STD of η_S near the Amazon River mouth due to freshwater discharge. Comparing the high STD of η_S in the western tropical Atlantic to the eastern tropical Atlantic, one can see the high STD of η_T off the west coast of Africa: two strong permanent coastal upwelling regions known as the Guinea Dome (12°N, 22°W) and the Angola Dome (10°S, 9°E) as shown in Figure 1a. In addition, we estimated the sea level height variation for the heat and the salt changes due to the undercurrent between 400 m and 1000 m. The STD was less than O (0.2 cm), which is not significant.

[10] We also studied the dispersal of Amazon water with SeaWiFS satellite images to illustrate the extent of front of the Amazon River outflow in the tropical Atlantic. Visible radiance backscattered out of the upper optical depth of the ocean is estimated by SeaWiFS. Nearshore, pigment concentrations are less reliable and are considered only qualitatively. *Muller-Karger et al.* [1988] showed that there are high pigment concentrations (5 mgm^{-3}), which reflect turbidity due to suspended sediment inshore of the 10 m isobath. Figures 2a and 2b show the annual mean Chl_a and DAC, which were computed from SeaWiFS data from September 1997 to July 2003. The correlation between Chl_a and DAC is over 96%. Chl_a and DAC are indirect evidence of freshwater discharge from the Amazon River and the coastal upwelling due to the high concentration of nutrients and suspended sediments. Figures 2a and 2b reveal the areas of high Chl_a and DAC related to freshwater discharge in the western tropical Atlantic as demonstrated using Figure 1b.

[11] Figure 2b shows DAC over the study area from SeaWiFS, which has an inverse relationship with the turbidity coefficient. The turbidity shows O (0.05 m^{-1}) in the offshore and over O (0.1 m^{-1}) in the near shore, which corresponds to 20 m and less than 10 m depth of light penetration, respectively. From this, one can see that the more freshwater discharge, the higher pigment concentration (Figure 2a) and the less light penetration (Figure 2b) in the associated region. It is worth noting that by comparing Figures 1b, 2a, and 2b, the western and eastern tropical Atlantic appear to have different dynamical processes [*Signorini et al.*, 1999]. There are strong salinity changes due to freshwater discharge in the western tropical Atlantic as shown in Figure 1b. While in the eastern tropical Atlantic, there are two permanent coastal upwelling regions: the Guinea Dome and the Angola Dome; and a possible third signal from the Congo River (5°S, 10°E) discharge. However, the features of the Congo River discharge do not appear in Figure 1b. In all likelihood,

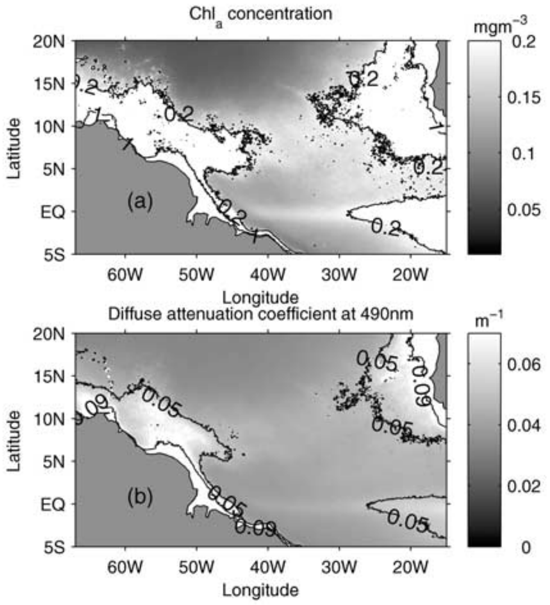

Figure 2. Annual mean from September 1997 to March 2004 of the Chlorophyll_a concentration and diffuse attenuation coefficient at 490 nm measured by SeaWiFS.

the extent of the area affected by the Congo River is not covered by this data set.

4. Long-Term Time Series of the Three Signals

[12] As mentioned in the Introduction, the most important tracer of the freshwater discharge in the ocean is the salinity. However, the coarse spatial sampling of salinity measurement throughout the global ocean can present difficulties in analysis. Since we do not have enough horizontal and vertical long-term time series of the salinity, we propose a method to estimate salt steric height variation using multi-sensor data. The sea level height anomaly derived from the altimeter data shows the total vertical water column, whereas the sea level height anomaly derived from long-term monthly mean XBT temperature measurements (η'_T) only shows the thermal expansion in the upper layer. For indirect evidence of freshwater discharge in the tropical Atlantic, we estimated the contribution of salinity variation to the altimeter measurements by removing thermal steric height anomaly and other dynamical signals, namely Ekman pumping and Sverdrup transport. Since the remnant signals are assumed to be a salt steric height due to salinity variation ($\Delta\eta'_S$) that corresponds to freshwater discharge from the Amazon River. We call this method; Integrated Multi-Sensor Data Analysis (IMSDA), i.e.,

$$\Delta\eta_S = \eta'_{Alt} - \left(\eta'_T + \eta'_W\right). \tag{3}$$

Where η'_W is the wind driven sea surface height variation. The η'_W through Sverdrup transport and through Ekman pumping, which are insignificant in the western tropical regions [*McClain and Firestone*, 1993; *Chambers et al.*, 1997]. For $\Delta\eta'_S$, we applied a three month box car filter. From this filtered data, it could be observed that the freshwater discharge increases the sea level height anomaly as shown in equation (2).

[13] In order to validate the Amazon River discharge using $\Delta\eta'_S$, we made a comparison with mean monthly SSS derived from averaging daily mean SSS from PIRATA mooring data in Figure 3a. As an example, the location 8°N, 38°W, where the North Equatorial Counter Current (NECC) passes through, will be highlighted [*Katz*, 1993]. This mooring site is the best choice from among the PIRATA sites to evaluate low-salinity due to entrainment of the Amazon plume water (~70%) resulting from NBC retroflection, and due to the NECC's carrying the Amazon plumes eastward into the North Atlantic during summer and fall. The remaining ~30% of the Amazon plume flows northwestward toward the Caribbean Sea [*Lentz*, 1995]. Moreover, by making a comparison at this mooring site, coastal upwelling can be avoided since it is located a large distance from the shoreline. Both time series show that the significant salinity variation occurs between October and November in every year. We also found that the precipitation obtained from the PIRATA data does not explain the minimum SSS at this site. The magnitude of $\Delta\eta'_S$ derived from IMSDA is reasonable when compared to both η'_S in equation (2) and measurements of error in the data. Using $\beta = 8 \times 10^{-4}$ ‰$^{-1}$, $\Delta S = 4$‰, and upper top layer (dz) as 20 m, η'_S can be easily obtained to an order of over 6 cm. For IMSDA, the accuracy of the altimeter is in the order of 2 cm [*Cheney et al.*, 1994], the instruments uncertainties of the XBT measurements are less than an order of ±0.1°C and ±1% of the depth [*White and Tai*, 1995]. Therefore, the salinity contribution into the sea level variation ($\Delta\eta'_S$ in equation (3)) derived from IMSDA as shown in Figure 3a is significant compared to the uncertainties.

[14] Chl_a and DAC can be also viewed as another tracer of freshwater discharge as explained in previous sections. The monthly mean Chl_a and DAC at 8°N, 38°W are plotted in Figure 3b. Both time series show that they are increased from September to October, and continue enhanc-

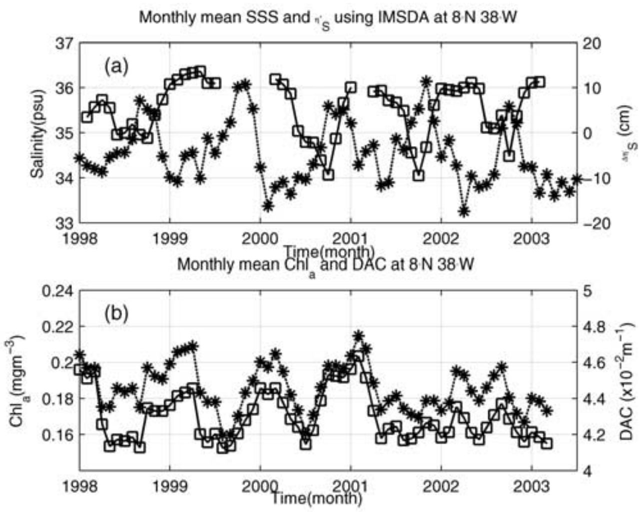

Figure 3. (a) Monthly mean long-term time series of SSS obtained from PIRATA data (squares with solid line), and salinity variation ($\Delta\eta'_S$, stars with dashed line) derived from IMSDA (equation (3)) at 8°N, 38°W. (b) The monthly mean Chl_a (squares with solid line), and DAC (stars with dashed line) at 8°N, 38°W.

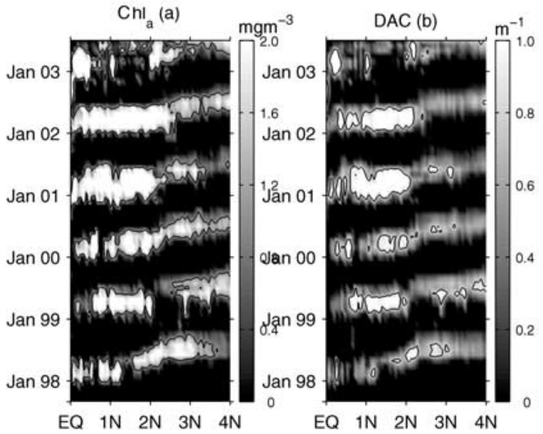

Figure 4. The latitude-time diagram of horizontal mean (a) Chl_a and (b) DAC anomaly measured by SeaWiFS. Contour in Figures 4a and 4b shows 0.8 mgm^{-3} and 1 m^{-1}, respectively. Horizontal mean was obtained by averaging values from the coast to 45°W.

ing during boreal winter. Both time series peak during boreal winter which can be explained by the Amazon plume being dominated by the NECC from summer to fall, and it being dominated by north east (NE) Trade wind from winter to spring [*Siedler et al.*, 1992; *Muller-Karger et al.*, 1988]. Thus, the increased Chl_a and DAC during boreal winter come from the east tropical Atlantic driven by NE Trade wind.

[15] Figures 4a and 4b show the latitude-time diagram of Chl_a anomaly and DAC anomaly, respectively. In order to illustrate variation of both properties clearly, we made both anomalies. Figures 4a and 4b show the similarities of the traveling features from the Amazon River toward north. However, there are stagnant areas before and after approximately 2°N. It seems both features do not reveal strong NBC, and hence it is not possible to estimate a traveling speed using Chl_a and DAC. The time lag of the high magnitude between 0°N and 4°N is about 3 to 5 months.

5. Discussion and Conclusion

[16] We demonstrated the variability of freshwater discharge from the Amazon River into the tropical Atlantic using SeaWiFS measurements, the IMSDA method, and mooring data. Estimating salinity variation using altimetry is based on the idea that altimetry measures the total change in sea level contributed by the entire water column, whereas XBT only measures temperature, from which only thermal steric height can be measured. Thus, the effects of temperature and salinity on the total sea level height anomaly can be separated. The minimum SSS from the PIRATA at 8°N, 38°W corresponds well with maximum $\Delta\eta_S$ derived from IMSDA every October. The time series of Chl_a and DAC reveal the Amazon plume starting in September and October at which time it was determined by the NECC, but later on it was dominated by NE Trade wind.

[17] The IMSDA method is particularly advantageous since satellite altimetry overcomes the difficulties of the conventional measurements of freshwater discharge. We believe that this method will help to estimate freshwater discharge from the Amazon River into the tropical Atlantic, which could be used in determining the freshwater budgets for a numerical modeling. Furthermore, the indirect signal of the salinity variation should be considered when making estimations of altimetry based global sea level height variation due to climate change and heat storage anomaly using altimetry.

[18] **Acknowledgment.** This research was supported partially by the National Aeronautics and Space Administration (NASA) through Grant NAG5-11773, and by the National Oceanic and Atmospheric Administration (NOAA) through grant NA17EC2449.

References

Baumgartner, A., and E. Reichel (1975), *The World Water Balance*, 179 pp., Elsevier, New York.

Chambers, D. P., B. D. Tapley, and R. H. Stewart (1997), Long-period ocean heat storage rates and basin-scale heat fluxes from TOPEX, *J. Geophys. Res.*, *102*, 10,525–10,533.

Cheney, R., L. Miller, R. Agreen, N. Doyle, and J. Lillibridge (1994), TOPEX/POSEIDON: 2 cm solution, *J. Geophys. Res.*, *99*, 24,555–24,563.

Dagg, M., R. Benner, S. Lohrenz, and D. Lawrence (2004), Transformation of dissolved and particulate materials on continental shelves influenced by large river: Plume processes, *Cont. Shelf Res.*, *24*, 833–858.

Hellweger, F. L., and A. L. Gordon (2002), Tracing Amazon River water into the Caribbean Sea, *J. Mar. Res.*, *60*, 537–549.

Katz, E. J. (1993), An interannual study of the Atlantic north equatorial countercurrent, *J. Phys. Oceanogr.*, *23*, 116–123.

Lentz, S. J. (1995), Seasonal variations in the horizontal structure of the Amazon plume interred from historical hydrographic data, *J. Geophys. Res.*, *100*, 2391–2400.

Levitus, S., R. Burgett, and T. P. Boyer (1994), *World Ocean Atlas 1994*, vol. 3, *Salinity*, *NOAA Atlas NESDIS*, 3, Natl. Oceanic and Atmos. Admin., Silver Spring, Md.

McClain, C. R., and J. Firestone (1993), An investigation of Ekman upwelling in the North Atlantic, *J. Geophys. Res.*, *98*, 12,327–12,339.

Muller-Karger, F. E., C. R. McClain, and P. L. Richardson (1988), The dispersal of the Amazon's water, *Nature*, *333*, 56–58.

Siedler, G., N. Zangenberg, and R. Onken (1992), Seasonal changes in the tropical Atlantic circulation: Observation and simulation of the Guinea Dome, *J. Geophys. Res.*, *97*, 703–715.

Signorini, S. R., R. G. Murtugudde, C. R. McClain, J. R. Christian, J. Picaut, and A. J. Busalacchi (1999), Biological and physical signatures in the tropical and subtropical Atlantic, *J. Geophys. Res.*, *104*, 18,367–18,382.

White, W. B., and C.-K. Tai (1995), Inferring interannual changes in global upper ocean heat storage from TOPEX altimetry, *J. Geophys. Res.*, *100*, 24,943–24,954.

B. Dzwonkowski, Y.-H. Jo, and X.-H. Yan, Center for Remote Sensing, Graduate College of Marine Studies, University of Delaware, Newark, DE 19716, USA. (xiaohai@udel.edu)

W. T. Liu, Jet Propulsion Laboratory, California Institute of Technology, Pasadena, CA 91109, USA.